AMERICAN SCIENTIFIC PUBLISHERS

Journal of Nanofluids
Vol. 6, pp. 457–465, 2017
(www.aspbs.com/jon)

ARTICLE

Boundary Layer Flow and Heat Transfer of Nanofluid Over Exponential Stretching Sheet with Effect of Slip and Nonlinear Thermal Radiation

Ch. Vittal[1,*], M. Chenna Krishna Reddy[1,2], and T. Vijayalaxmi[1,2]

[1]*Department of Mathematics, Osmania University, Hyderabad 500007, Telangana, India*
[2]*Mahaboobnagar Vidya Samithi Government Arts and Science UG, PG College Christianpally, Mahaboobnagar 509001, Telangana, India*

The boundary layer flow, heat and mass transfer of a nanofluid with boundary slip condition for velocity, thermal and solutal slip, and nonlinear thermal radiation has been investigated numerically over an exponential stretching sheet with suction. The profiles for the velocity, temperature and nanoparticle concentration depends on parameters viz. temperature ratio parameter θ_w, radiation parameter *Nr*, suction parameter *s*, velocity slip parameter λ, thermal slip parameter δ, concentration slip parameter α, Prandtl number *Pr*, Lewis number *Le*, Brownian motion parameter *Nb* and thermophoresis parameter *Nt*. Similarity transformation is used to convert the governing non-linear boundary-layer equations into coupled higher order non-linear ordinary differential equations. These equations are numerically solved by using an implicit finite difference method known as Keller-Box method. An analysis has been carried out to reveals the effects of governing parameters corresponding to various physical conditions. Numerical results and Graphical representation are obtained for distributions of velocity, temperature and concentration, as well as, for the skin friction, local Nusselt number and local Sherwood number for several values of governing parameters. The result reveals that velocity decreases with increase of velocity slip, suction. Temperature decreases with the increase of thermal slip, suction but increases with temperature ratio parameter as well as radiation parameter. Nanoprticle concentration decreases with increase of concentration slip, suction. A comparison with previous results available in the literature has been done and we found a good conformity with it. The numerical values of skin friction, Nusselt number and Sherwood number are presented in tables.

KEYWORDS: Nonlinear Thermal Radiation, Nanofluid, Exponential Stretching Sheet, Slip Conditions, Suction.

1. INTRODUCTION

Nanofluid introduced by Choi et al.,[1] gives the fluid contains of nano-sized particles (diameter of 1 to 100 nm) are suspended in a base fluid like water, ethylene glycol, propylene glycol, etc. Addition of high thermally conductive metallic nano particles, like silver, copper, aluminium, silicon improves thermal conductivity of such mixtures, thereby enhance the overall energy transport capability. It has been found that nanofluids have a potential to increase the thermal conductivity as well as convective heat transfer performance of the base fluid. One of the possible mechanisms for anomalous increase in the thermal conductivity of nanofluids is the Brownian motion of the nanoparticles within the base fluids. This attractive characteristic of nanofluids creates an impressive for wide application.[2,3] Nanofluids became the next-generation heat transfer fluids and their superior heat transfer features are better than that of any other ordinary fluids. Khan and Pop[4] studied the phenomenon of nanofluid over a stretching sheet for laminar boundary layer flow. The nanofluid flow over an exponentially stretching sheet was introduced by Nadeem and Lee.[5] The laminar boundary layer flow of a nanofluid over a nonlinear stretching sheet is extended by Rana and Bhargava.[6] Rahman and Eltayeb[7] extend the radiative heat transfer in a hydromagnetic nanofluid over a nonlinear stretching surface. Cortell et al.[8] explained the boundary layer flow and heat transfer of fluid under the consideration of thermal radiation and viscous dissipation over a nonlinear stretched sheet. The boundary layer flow over a permeable moving flat plate under the effect of viscous dissipation and thermal radiation by considering of few nanofluids is studied by Motsumi and Makinde.[9] Heat transfer over nonlinear stretching and shrinking sheets under the influence of magnetic field, thermal radiation and viscous dissipation by considering copper, alumina,

*Author to whom correspondence should be addressed.
Email: vittalch1006@gmail.com
Received: 1 November 2016
Accepted: 18 December 2016

and titanium oxide nanoparticles was examined by Pal et al.[10] Later, Nandy and Pop[11] extended the study of MHD boundary layer stagnation flow and heat transfer over a shrinking sheet incorporating the two component model under the effect of radiation. Rashidi et al.[12] have also investigated the combined effect of magnetic field and thermal radiation over a vertical stretching sheet for two dimensional water based nanofluid flow. Mustafa et al. studied[13] the boundary layer flow of a nanofluid over an exponentially stretching sheet to the case of a permeable shrinking sheet with the second order velocity slip in the presence of zero normal flux of the nanoparticles at the boundary. Several authors have studied the flow and heat transfer of a viscous (regular) fluid over an exponentially stretching surface.[14–17]

Boundary layer flow over a stretching surface with velocity slip boundary conditions is an important type of flow and heat transfer occurring in several engineering applications. In these types of transport phenomena the equations corresponding to continuum equations of momentum and energy are still governed by the Navier-Stokes equations, but the effects of the walls are taken into account by using appropriate boundary conditions. No-slip condition is inadequate for most non-Newtonian liquids, as some polymer melt often shows microscopic wall slip and that has a controlling influence by a nonlinear and monotone relation between the slip velocity and the traction. It is known that, a viscous fluid normally sticks to boundary and there is no slip of the fluid relative to the boundary. However, in some situations there may be a partial slip between the fluid and the boundary. For such fluid, the motion is still governed by the Navier Stokes equations, but the usual no-slip condition at the boundary is replaced by the slip condition. Partial velocity slip may occur on the stretching boundary when the fluid is particulate such as emulsions, suspensions, foams and polymer solutions. In various industrial processes, slip effects can arise at the boundary of the pipes, walls, curved surfaces etc. A boundary layer slip flow problem arises in polishing of artificial heart valves and internal cavities. Recently many authors obtained analytical and numerical solutions for boundary layer flow and heat transfer due to a stretching sheet with slip boundary conditions.[18–25]

Heat transfer, influenced by thermal radiation has applications in many technological processes, including nuclear power plants, gas turbines and various propulsion devices for aircraft, missiles, satellites and space vehicles. A linear radiation is not valid for high temperature difference and also dimensionless parameter that is used in the linearized Rosseland approximation is only the effective Prandtl number, whereas in case of non-linear approximation the problem is governed by three parameters, Prandtl number, the radiation parameter and the temperature ratio parameter. First time in the literature, Pantokratoras[26] investigated the effect of linear/nonlinear Rosseland radiation on steady laminar natural convection along a vertical isothermal plate by using a new radiation parameter called film radiation parameter. Hayat et al.[27] analysed the effect of nonlinear thermal radiation and constant applied magnetic field on magnetohydrodynamic three-dimensional flow of couple stress nanofluid and viscous nanofluid in the presence of thermophoresis and Brownian motion effects. Shehzad et al.[28] have explored the characteristics of thermophoresis and Brownian motion in magnetohydrodynamic three-dimensional flow of nano-Jeffrey fluid in the presence of nonlinear thermal radiation. Recently Vijayalaxmi et al.[29] deliberate the effect of nonlinear thermal radiation on boundary layer flow of viscous fluid over nonlinear stretching sheet with injection/suction. Moreover Krishnamurthy[30] and co-authors analyze the nonlinear thermal radiation and slip effects on boundary layer flow and heat transfer of suspended nanoparticles over a stretching sheet embedded in porous medium with convective boundary conditions. Also Mabood et al.[31] studied the numerical study of unsteady convective boundary layer flow of Maxwell fluid with nonlinear thermal radiation.

Motivated by the above literature we studied the effects of nonlinear thermal radiation and slips on boundary layer flow of nanofluid over exponential sheet.

2. FLOW ANALYSIS AND MATHEMATICAL FORMULATION

Consider a two dimensional steady and incompressible viscous flow of a nanofluid past an exponential sheet coinciding with the plane $y = 0$. The nanofluid flows at $y = 0$, where y is the coordinate normal to the surface. The flow is confined to $y > 0$. Two equal and opposite forces are applied along the x-axis so that the wall is stretched keeping the origin fixed. The stretching surface temperature and the nanoparticles fraction are deemed to have a constant value T_w and C_w, respectively. The ambient fluid temperature and nanoparticles fraction have constant value T_∞ and C_∞, respectively. The coordinate system and flow regime is illustrated as shown in the Figure 1.

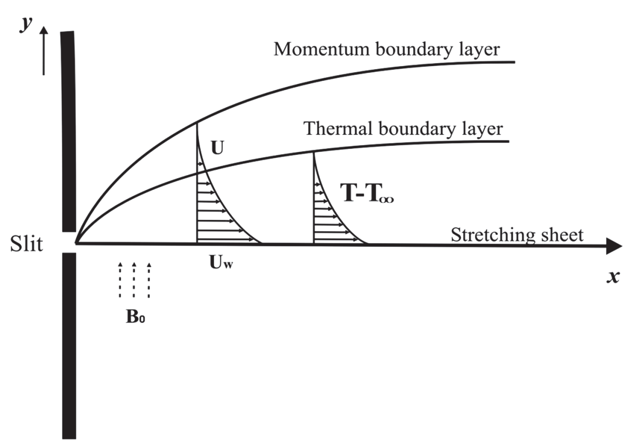

Fig. 1. Physical model and coordinate system.

The governing equations of continuity, momentum, thermal energy and nanoparticles equations governing such type of flow are written as,

$$\frac{\partial u}{\partial x}+\frac{\partial v}{\partial y}=0 \tag{1}$$

$$u\frac{\partial u}{\partial x}+v\frac{\partial u}{\partial y}=\nu\frac{\partial^2 u}{\partial y^2} \tag{2}$$

$$u\frac{\partial T}{\partial x}+v\frac{\partial T}{\partial y}=\frac{k}{\rho c_p}\frac{\partial^2 T}{\partial y^2}-\frac{1}{\rho c_p}\frac{\partial q_r}{\partial y}+\tau\left[D_B\frac{\partial C}{\partial y}\frac{\partial T}{\partial y}+\frac{D_T}{T_\infty}\left(\frac{\partial T}{\partial y}\right)^2\right] \tag{3}$$

$$u\frac{\partial C}{\partial x}+v\frac{\partial C}{\partial y}=D_B\frac{\partial^2 C}{\partial y^2}+\frac{D_T}{T_\infty}\frac{\partial^2 T}{\partial y^2} \tag{4}$$

where u and v are the components of velocity respectively in the x and y directions, $\nu=\mu/\rho$ is the kinematic viscosity, ρ is the fluid density (assumed constant), μ is the coefficient of fluid viscosity, qr is the radiative heat flux, cp is the specific heat at constant pressure, k is the thermal conductivity of the fluid, D_B is the Brownian diffusion coefficient and D_T is the thermophoresis diffusion coefficient. $\tau=(\rho C)_p/(\rho C)_f$ is the ratio between the effective heat capacity of the nanoparticle material and heat capacity of the fluid.

Unlike the linearized Rosseland approximation, we use nonlinear Rosseland diffusion approximation from which one can obtain results for both small and large differences between T_w and T_∞. Using Rosseland[32] approximation for radiation, the radiative heat flux is simplified as,

$$q_r=-\frac{4\sigma^*}{3k^*}\frac{\partial T^4}{\partial y} \tag{5}$$

We assume that the temperature differences within the flow region, namely, the term T^4 can be expressed as a linear function of temperature. The best linear approximation of T^4 is obtained by expanding it in a Taylor series about T_∞ and neglecting higher order terms. That is

$$T^4\cong 4T_\infty^3T-3T_\infty^4 \tag{6}$$

using Eq. (8) into Eq. (7) the modified equation of (3) is

$$q_r=\frac{-4\sigma^*}{3k^*}\frac{\partial}{\partial y}(4T_\infty^3-3T_\infty^4)=\frac{-16\sigma^*T_\infty^3}{3k^*}\frac{\partial T}{\partial y}$$

and

$$\frac{\partial q_r}{\partial y}=\frac{-16\sigma^*T_\infty^3}{3k^*}\frac{\partial^2 T}{\partial y^2} \tag{7}$$

$$u\frac{\partial T}{\partial x}+v\frac{\partial T}{\partial y}=\frac{\partial}{\partial y}\left[\left(\alpha+\frac{16\sigma^*T_\infty^3}{3k^*(\rho c)_f}\right)\frac{\partial T}{\partial y}\right]+\tau\left\{D_B\frac{\partial C}{\partial y}\frac{\partial T}{\partial y}+\frac{D_T}{T_\infty}\left(\frac{\partial T}{\partial y}\right)^2\right\} \tag{8}$$

The appropriate boundary conditions for the problem are given by[18]

$$\begin{gathered}u=U+N\nu\frac{\partial u}{\partial y},\quad v=-V(x),\quad T=T_w+D\frac{\partial T}{\partial y},\\ C=C_w+E\frac{\partial C}{\partial y}\quad\text{at } y=0\\ u\to 0,\quad T\to 0,\quad C\to 0\quad\text{as } y\to\infty\end{gathered} \tag{9}$$

Here $U=U_0e^{x/L}$ is the stretching velocity, $T_w=T_0e^{x/(2L)}$ is the temperature at the sheet and $C_w=C_0e^{x/(2L)}$. U_0, T_0, and C_0 are the reference velocity, temperature and concentration respectively, $N=N_1e^{-x/(2L)}$ is the velocity slip factor which changes with x, N_1 is the initial value of velocity slip factor, $D=D_1e^{-x/(2L)}$ is the thermal slip factor which also changes with x, D_1 is the initial value of thermal slip factor and $E=E_1e^{-x/(2L)}$ is the solutal slip factor which also changes with x, E_1 is the initial value of solutal slip factor. The no-slip case is recovered for $N=0=D=E$. $V(x)$ greater than zero is the velocity of suction and $V(x)$ less than zero is the velocity of blowing, $V(x)=V_0e^{x/(2L)}$, a special type of velocity at the wall is considered. V_0 is the initial strength of suction.

Introducing the similarity variables as

$$\eta=\sqrt{\frac{U_0}{2\nu L}}e^{x/(2L)}y,\quad u=U_0e^{x/L}f^1(\eta),$$

$$v=-\sqrt{\frac{U_0\nu}{2L}}e^{x/(2L)}\{f(\eta)+\eta f^1(\eta)\},$$

$$T=T_\infty(1+(\theta_w-1)\theta(\eta)),\quad \phi(\eta)=\frac{C-C_\infty}{C_w-C_\infty}$$

where $\theta_w=T_w/T_\infty$, $\theta_w>1$, the temperature ratio parameter Shehzad et al.[33] and upon substitution of (10) in Eqs. (2)–(4) the governing equations reduce to

$$f'''+ff''-2(f')^2=0 \tag{11}$$

$$(1+Nr(1+(\theta_w-1)\theta)^3\theta')'+Pr(f\theta'-f'\theta)+Nb\theta'\varphi'+Nt(\theta')^2=0 \tag{12}$$

$$\varphi''+Le(f\varphi'-f'\varphi)+\frac{Nt}{Nb}\theta''=0 \tag{13}$$

and the boundary conditions take the following form:

$$\begin{gathered}f'=1+\lambda f'',\quad f=s,\quad \theta=1+\delta\theta',\\ \varphi=1+\alpha\varphi',\quad\text{at } \eta=0\\ f'\to 0,\quad \theta\to 0,\quad \varphi\to 0,\quad\text{as } \eta\to\infty\end{gathered} \tag{14}$$

where the prime denotes differentiation with respect to η, $\lambda=N_1\sqrt{U_0/(2\nu L)}e^{x/(2L)}$ is the velocity slip parameter, $\delta=D_1\sqrt{U_0/(2\nu L)}e^{x/(2L)}$ is the thermal slip parameter and $\alpha=E\sqrt{U_0/(2\nu L)}e^{x/(2L)}$ is the concentration slip

parameter, $S = V_0/(\sqrt{(U_0\nu)/(2L)})$ the suction (or blowing) parameter, $Nr = (16\sigma^* T_\infty^3)/(3kk^*)$ is the radiation parameter, $Pr = (\mu c_p)/k$ is the prandtl number, $Le = \nu/D_B$ is the Lewis number, $Nt = (\rho_p c_p)/(\rho c(C_w - C_\infty))$ thermophoresis parameter, $Nb = (D_B T_\infty (C_W - C_\infty))/(D_T(T_W - T_\infty))$ Brownian motion parameter.

The quantities of practical interest, in this study, are the local skin friction Cf_x, Nusselt number Nu_x and the Sherwood number Sh_x which are defined as

$$C_f = \frac{\tau_w}{\rho u_w^2}, \quad Nu_x = \frac{xq_w}{k(T_w - T_\infty)}, \quad Sh_x = \frac{xq_m}{D_B(C_w - C_\infty)} \tag{19}$$

where τ_w is shear stress at wall, q_w is the heat flux and q_m is the mass flux at the surface which are given below:

$$\tau_w = \mu\left(\frac{\partial u}{\partial y}\right)_{y=0}, \quad q_w = -\left(k + \frac{16\sigma^* T_\infty^3}{3k^*}\right)\left(\frac{\partial T}{\partial y}\right)_{y=0}, \quad q_m = -D_B\left(\frac{\partial C}{\partial y}\right)_{y=0} \tag{20}$$

Substituting Eq. (10) into Eqs. (19), (20), we obtain

$$C_f Re^{1/2} = f''(0), \quad Nu_x Re^{-1/2} = -(1 + Nr\theta_w^3)\theta'(0), \quad Sh_x Re^{-1/2} = -\phi'(0) \tag{21}$$

3. NUMERICAL METHODS

The ordinary differential Eqs. (11)–(13) with the boundary conditions of Eq. (14) are solved numerically by using of Keller-Box method, as revealed by Ref. [34] the following few steps are involved to achieve Numerical solutions:

- Reduce the above mentioned higher order ordinary differential equations into a system of first order ordinary differential equations;
- Write the finite differences for the first order equations.
- Linearize the algebraic equations by Newton's method, and write them in matrix–vector form; and
- Solve the linear system by the block tri-diagonal elimination technique.

To get the accuracy of this method the appropriate initial guesses have been chosen. The following initial guesses are chosen.

$$f_0(\eta) = s + \frac{1}{1+\lambda}(1 - e^x), \quad \theta_0(\eta) = \left(\frac{1}{1+\delta}\right)e^{-x}, \quad \phi_0(\eta) = \left(\frac{1}{1+\alpha}\right)e^{-x}$$

The choices of the above initial guesses depend on the convergence criteria and the transformed boundary conditions of Eq. (14). The step size 0.01 is used to obtain the numerical solution with four decimal place accuracy as the criterion of convergence.

4. RESULTS AND DISCUSSION

The boundary layer flow and heat transfer of a nanofluid with velocity slip, temperature jump, solutal boundary slip condition, suction and nonlinear thermal radiation has been investigated numerically over an exponential stretching sheet. The numerical solutions are obtained for velocity, temperature and concentration profiles for different values of governing parameters. The obtained results are displayed through Figures 2–16 for velocity, temperature and

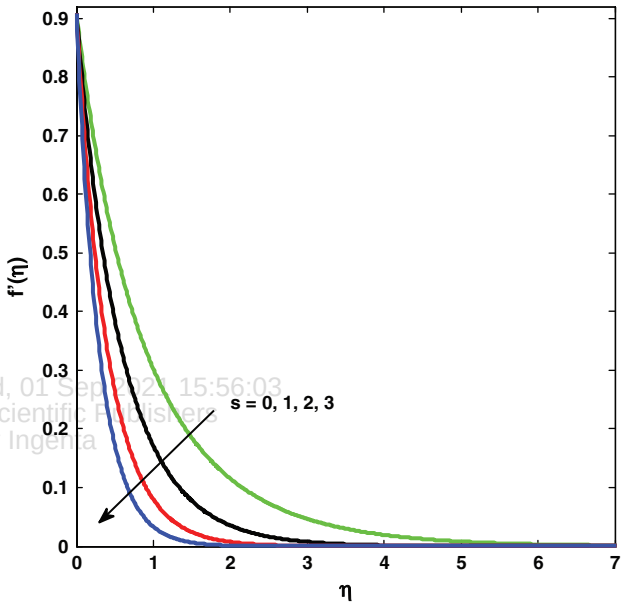

Fig. 2. Effect of s on velocity profile.

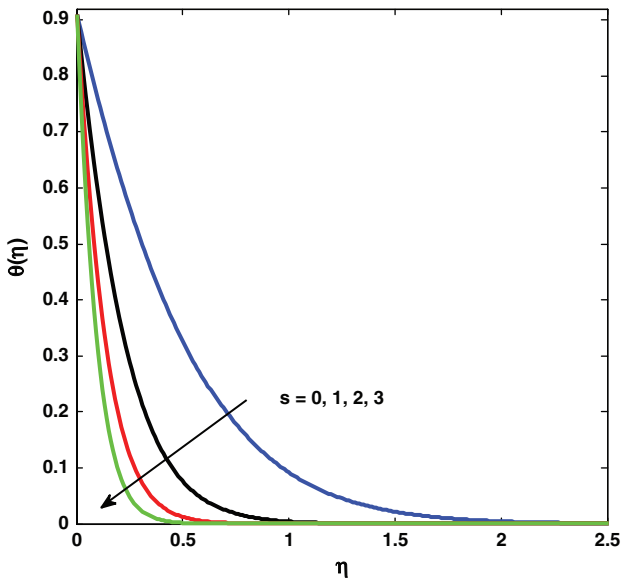

Fig. 3. Effect of s on temperature profile.

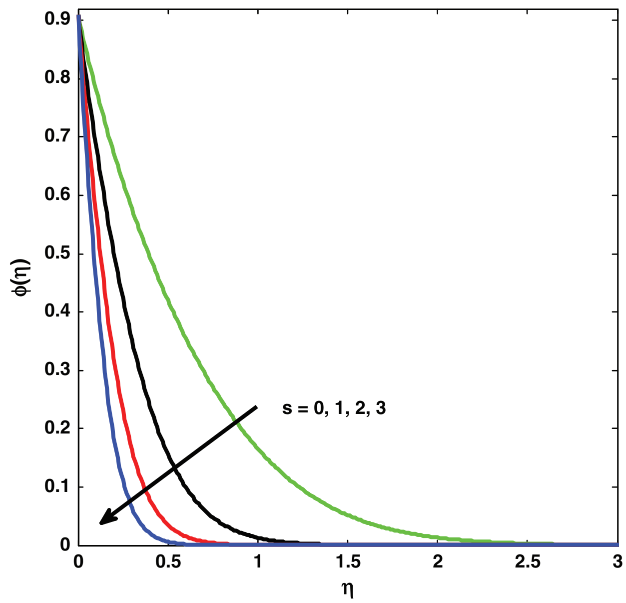

Fig. 4. Effect of s on concentration profile.

concentration profiles, respectively. In the simulation the default values of the parameters are considered as $Nr = Nb = Nt = 0.5$, $Le = 5$, $Pr = 6.8$, $s = 0.5$, $\lambda = 0.1$, $\delta = 0.1$, $\alpha = 0.1$, $\theta_w = 1.2$, unless otherwise specified.

The effect of suction parameter 's' on the velocity profile for an exponential stretching surface is presented in Figure 2 in presence of surface slip. It is observed from the figure that velocity distribution across the boundary layer decreases with an increase in suction parameter s. Thus, the suction reduces the thickness of hydrodynamic boundary layer, the effect is reverse in the case of injection. In Figure 3 the influence of the suction parameter 's' on the temperature profiles is depicted. It can, easily, be seen

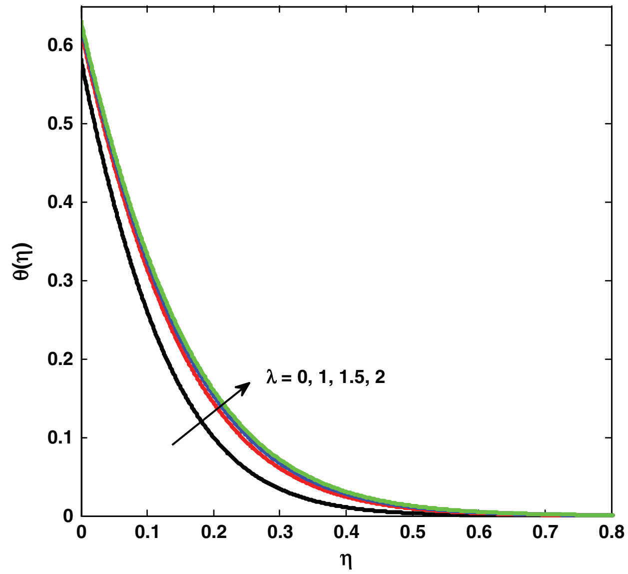

Fig. 6. Effect of λ on temperature profile.

from the figure that the temperature distribution across the boundary layer decreases with increasing the values of $s > 0$ in the presence of thermal slip and hence the thickness of the thermal boundary layer decreases. The suction parameter 's' has a strong influence on the concentration profile as it is shown in Figure 4. As the values of suction parameter s increase, concentration graph decreases and the concentration boundary layer thickness decreases.

Figure 5 illustrates the variation of the dimensionless velocity component $f'(\eta)$ for various values of the velocity slip parameter λ. From the figure, it is clear that the velocity of the fluid near the boundary layer region decreases by increasing slip parameter. If the slip

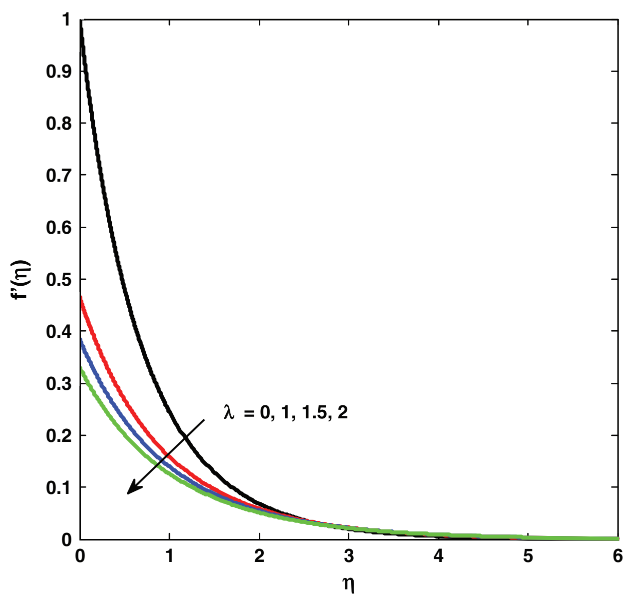

Fig. 5. Effect of λ on velocity profile.

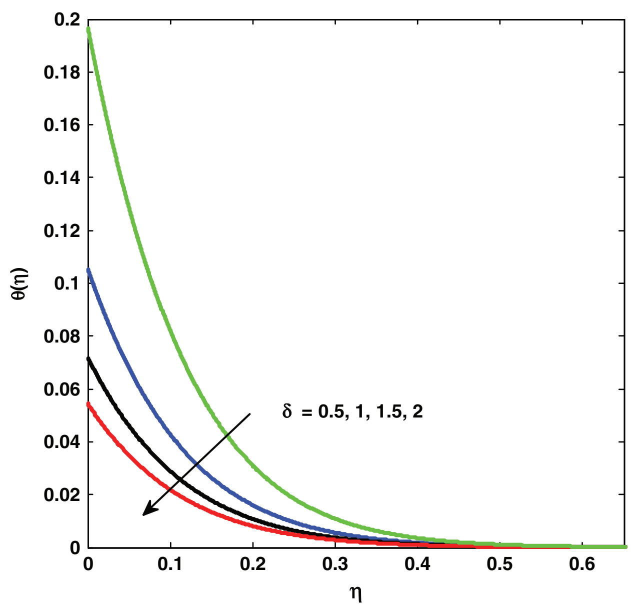

Fig. 7. Effect of δ on temperature profile.

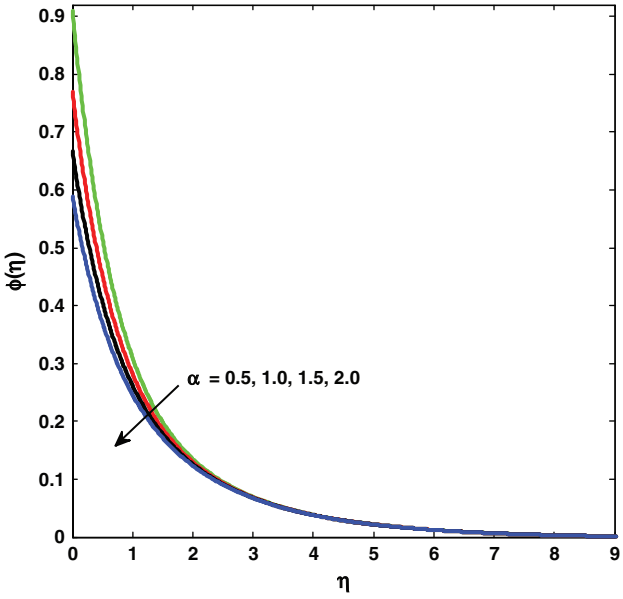

Fig. 8. Effect of α on concentration profile.

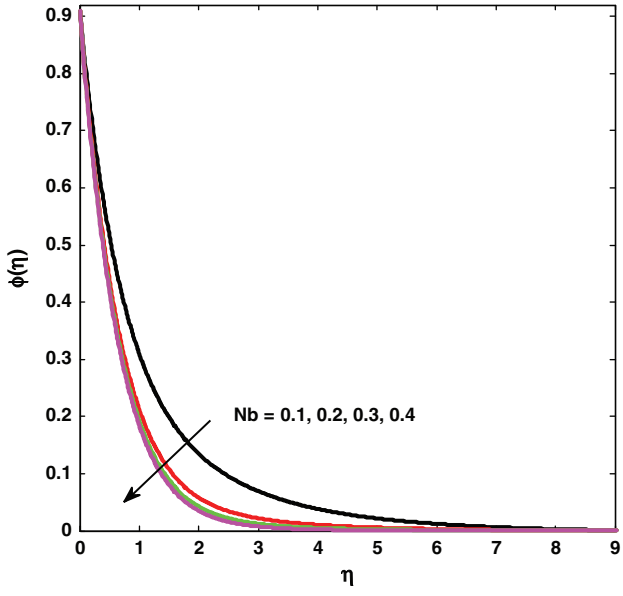

Fig. 10. Effect of *Nb* on concentration profile.

parameter increases, the slip at the surface wall is also increases. As a result it reaches to a smaller amount of diffusion due to the stretching surface into the fluid. In the case of temperature profile we observe the opposite result. i.e., from Figure 6 with the increasing values of velocity slip the temperature profile is increases. The influence of thermal slip on the temperature profile is shown in Figure 7 which describes that the fluid temperature decreases on increasing thermal slip parameter δ in the boundary layer region and, as a consequence, thickness of the thermal boundary layer decreases. From Figure 8 we can observe the variation of concentration with respect to solutal slip parameter α. As it can be seen from the graph, increasing in the concentration slip parameter α, the concentration profile is decreasing.

Temperature and nanoparticle volume fraction variation against different values of *Nb* and *Nt* are depicted respectively, as in Figures 9–12. We can see that the temperature profiles are increasing function of *Nb*, whereas nanoparticle volume fraction is a decreasing one. This may be due to the fact that as Brownian motion parameter (*Nb*) decreases the mass transfer of a nanofluid. Further, both temperature and nanoparticle volume fraction profiles increases for increasing values of *Nt*.

The effect of Prandtl number *Pr* on the heat transfer process is shown by the Figure 13. This figure reveals that

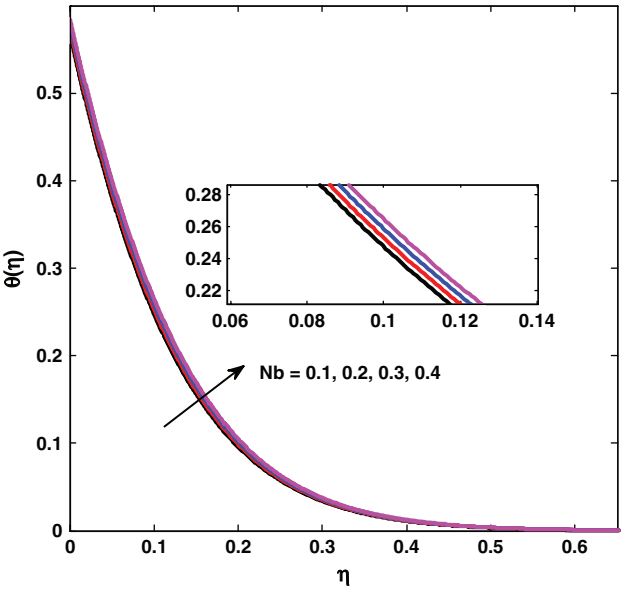

Fig. 9. Effect of *Nb* on temperature profile.

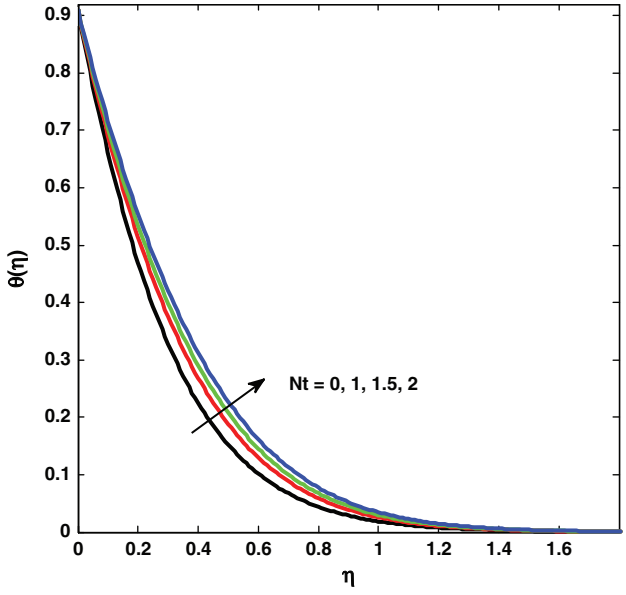

Fig. 11. Effect of *Nt* on temperature profile.

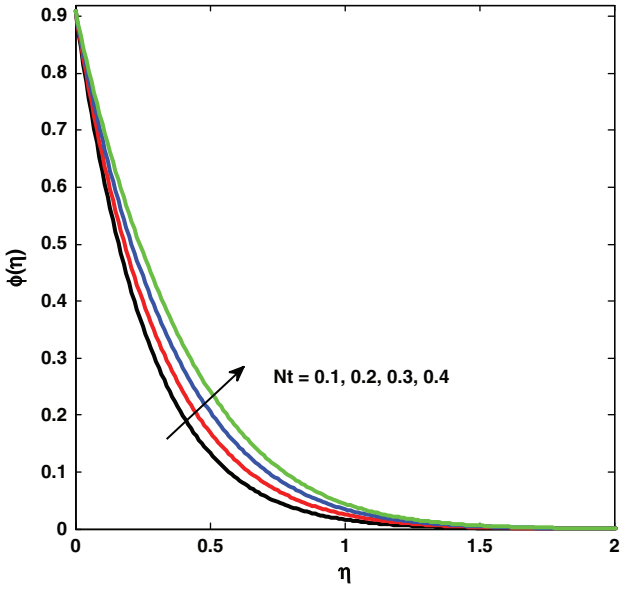

Fig. 12. Effect of Nt on concentration profile.

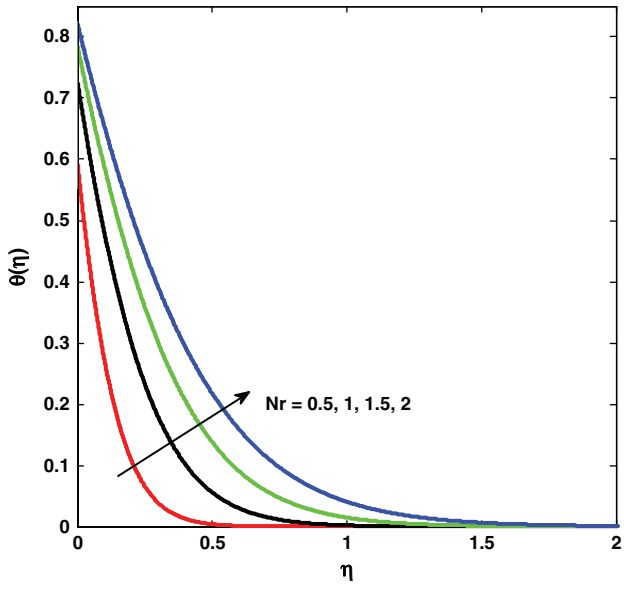

Fig. 14. Effect of Nr on temperature profile.

as an increase in Prandtl number Pr, the temperature field decreases. It is obvious that, an increase in the values of Pr reduces the thermal diffusivity, therefore thermal boundary layer thickness is a decreasing function of Pr.

The effect of radiation parameter on temperature is depicted as in Figure 14. A critical observation shows that, the temperature profile increases with increase in Nr. This is because; an increase in the radiation parameter provides more heat to fluid that causes an enhancement in the temperature and thermal boundary layer thickness. Figure 15 illustrates the effect of temperature ratio parameter (θ_w) on temperature profiles. From this plot, one can notice that, an increase in temperature ratio parameter increases the thermal state of the fluid, and it results in increase of temperature profiles.

As it is noticed from Figure 16, as Lewis number increases, the mass diffusivity decreases so it decreases the concentration field. Due to the increase in mass transfer rate the concentration boundary layer thickness decreases.

Finally, a comparison is done with previous results as it is shown in Tables I and II, for the numerical values of the local Nusselt number—$\theta'(0)$ for several values of prandlt number in the absence and presence of thermal radiation. And it is in excellent agreement with the result published in Magyari and Keller,[35] Bidin and Nazar,[36] El-Aziz,[37] Ishak,[38] Mukhopadhyay,[39] Nadeem.[40]

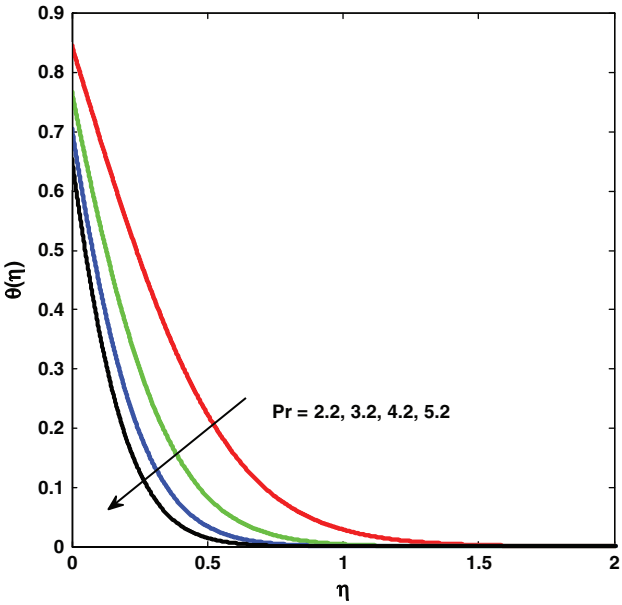

Fig. 13. Effect of Pr on temperature profile.

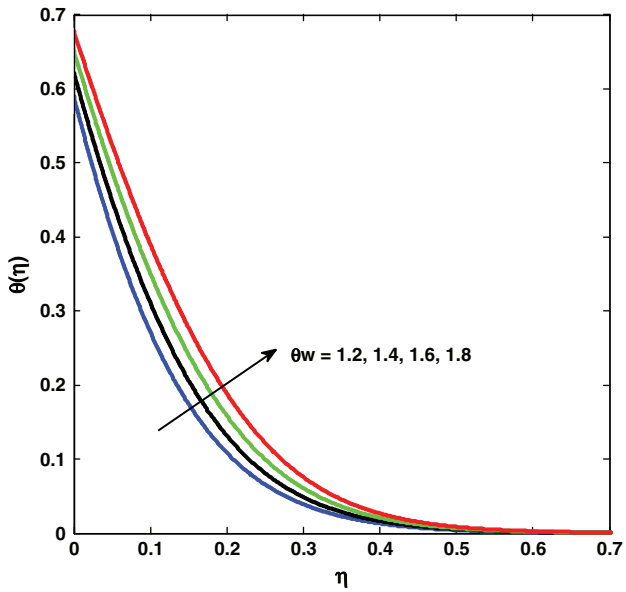

Fig. 15. Effect of θ_w on temperature profile.

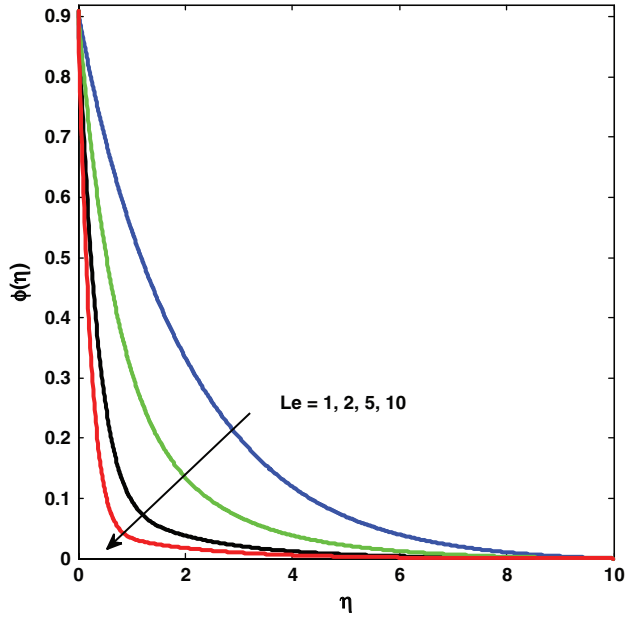

Fig. 16. Effect of *Le* on concentration profile.

Table I. Values of $[-\theta^1(0)]$ for several values of prandlt number in the absence of thermal radiation.

Pr	Magyari and Keller	Bidin and Nazar	El-Aziz	Ishak	Swathi Mukhopadhyaya	Present work
1	0.954782	0.9547	0.954785	0.9548	0.9547	0.9548
2		1.4714		1.4715	1.4714	1.4715
3	1.869075	1.8691	1.869074	1.8691	1.8691	1.8691
5	2.500135		2.500132	2.5001	2.5001	2.5001
10	3.660379		3.660372	3.6604	3.6603	3.6605

Table III presents the variation of the skin friction coefficient in relation to suction s and velocity slip parameter λ. On observing this table, as the values of suction parameter increase, the values of skin friction coefficient increase. However, the skin friction coefficient decreases as the values of velocity slip parameters λ increase. Table IV shows the local Nusselt number—$\theta'(0)$ and Sherwood number—$\Phi'(0)$ for different values of Prandtl number Pr, nonlinear thermal radiation Nr, temperature ratio parameter θ_w, thermal slip parameter δ, concentration parameter α, Lewis number Le, thermophoresis parameter Nt, Brownian motion parameter Nb. It is possible to see that as the values of Prandtl number increase, the heat transfer rate (local Nusselt number) is increase, but when other values as indicated in Table IV increases, the local Nusselt number decreases. Also we can observe the variation of the mass transfer rate i.e., Sherwood number from this Table.

Table III. Computed values of skin friction coefficient for various parameters.

λ	s	cf_x	Nu_x	Sh_x
0.1		1.272326	4.103301	1.997802
0.2		1. 090869	4.045301	1.962294
0.3		0.958442	3.998691	1.933849
	0	1.079888	2.414738	1.033211
	1	1.495410	5.482468	2.871916
	2	1.995011	7.081058	3.975494

Table IV. Computed values of Local nusselt number for various values of parameters.

Pr	Nb	Nt	Le	Nr	θ_w	δ	α	Nu_x	Sh_x
0.7								0.155488	7.084293
1								0.321825	6.106282
2								1.352028	2.874922
	0.5							4.103301	−1.997802
	1							3.777533	0.327522
	2							2.837826	1.943991
		0.4						4.106864	−1.194977
		1						4.085446	−5.990428
		2						4.049533	−13.86754
			1					4.309984	−3.800471
			2					4.260918	−3.366085
			10					3.798173	0.547360
				0.5				4.103301	−1.997802
				1				2.769484	0.154709
				1.5				2.158889	1.295794
					1.2			4.103301	−1.997802
					1.4			3.781260	−1.529999
					1.6			3.487046	−1.093441
						0.1		4.103301	−1.997802
						0.2		3.002346	−1.565401
						0.3		2.338522	−1.252625
							0.1	4.103301	−1.997802
							0.2	4.099772	−1.979439
							0.3	4.096305	−1.961406

Table II. Values of $[-\theta^1(0)]$ for several values of prandlt number in the presence of thermal radiation.

	Bidin and Nazar (For $K = 0.5, 1$)		Nadeem et al. (For $R = 0.5, 1$)		Swathi Mukhopadhyaya (For $R = 0.5, 1$)		Present work (For $R = 0.5, 1$)	
Pr	0.5	1	0.5	1	0.5	1	0.5	1
1	0.9547	0.5315	0.680	0.534	0.6765	0.5315	0.6775	0.5354
2	1.4714	0.8627	1.073	0.863	1.0734	1.0734	1.0735	0.8629
3	1.8691	1.1214	1.381	1.121	1.3807	1.3807	1.3807	1.1214

5. CONCLUSIONS

A numerical study was investigated for the nonlinear thermal radiative boundary layer flow and heat transfer of nanofluids over an exponential stretching sheet with slip conditions, suction with the help of an implicit finite difference method known as Keller-Box method. A parametric study is performed to explore the effects of various governing parameters on the fluid flow and heat transfer characteristic. Following conclusions give the brief results of the present study.

(1) Velocity slip parameter λ reduces the thickness of momentum boundary layer and increase the thermal boundary layer thickness.

(2) Velocity profile decrease with increase in suction parameter s.

(3) Prandtl number Pr, thermal slip parameter δ, suction parameter s reduces the temperature profile.

(4) The temperature increases with an increase in nonlinear thermal radiation parameter Nr, temperature ratio parameter θ_w, thermophoresis parameter Nt, Brownian motion parameter Nb.

(5) Concentration profile decreases with an increase in Lewis number Le, Brownian motion parameter Nb, thermal slip parameter δ, concentration slip parameter α, suction s and radiation Nr but increases with an increase in thermophoresis parameter Nt.

References and Notes

1. S. U. S. Choi, *Dev. Appl. Non-Newton Flows* 66, 99 (**1995**).
2. J. Buongiorno and L. W. Hu, *Proceedings of ICAPP 2005*, Seoul (**2005**), Paper no. 5705, pp. 15–19.
3. K. N. Shukla, A. B. Solomon, and B. C. Pillai, *J. Ther. Heat Transfer* 24, 796 (**2010**).
4. W. A. Khan and I. Pop, *Int. J. Heat Mass Trans.* 53, 2477 (**2010**).
5. S. Nadeem and C. Lee, *Nanoscale Res. Lett.* 7, 94 (**2012**).
6. P. Rana and R. Bhargava, *Commun. Nonlin. Sci. Numer. Simul.* 17, 212 (**2012**).
7. M. M. Rahmann and I. A. Eltayeb, *Meccanica* 48, 601 (**2013**).
8. R. Cortell, *Phys. Lett. A* 372, 631 (**2008**).
9. T. G. Motsumi and O. D. Makinde, *Phys. Script* 86, 045003 (**2012**).
10. D. Pal, G. Mandal, and K. Vajravelu, *Int. J. Heat Mass Trans.* 65, 481 (**2013**).
11. S. K. Nandy and I. Pop, *Int. Comm. Heat Mass Trans.* 53, 50 (**2014**).
12. M. M. Rashidi, N. V. Ganesh, A. K. A. Hakeem, and B. Ganga, *J. Mol. Liq.* 198, 234 (**2014**).
13. M. Mustafa, T. Hayat, and S. Obaidat, *Int. J. Num. Met. Heat Fluid Flow* 23, 945 (**2013**).
14. S. Nadeem, T. Hayat, M. Y. Malik, and S. A. Rajput, *Natur. Forsch.* 65A, 1 (**2010**).
15. S. Nadeem and C. Lee, *Nanoscale Res. Lett.* 7, 94 (**2012**).
16. K. Bhattacharyya, *Chin. Phys. Lett.* 28, 074701 (**2011**).
17. K. Bhattacharyya and K. Vajravelu, *Comm. Nonlinear Sci. Numer. Simul.* 17, 2728 (**2012**).
18. Wubshet Ibrahim and Bandari Shankar, *Comput. Fluids* 75, 1 (**2013**).
19. Wubshet Ibrahim1 and Bandari Shanker, *Heat Transfer—Asian Res.* 43, 5 (**2014**).
20. Eshetu Haile Gorfie and Bandari Shankar, *J. Progressive Res. in Mathematics (JPRM)* 5, 444 (**2015**).
21. T. Vijayalaxmi and Bandari Shankar, *J. Nanofluids* 5, 696 (**2016**).
22. T. Vijayalaxmi and Bandari Shankar, *J. Nanofluid* 5, 826 (**2016**).
23. V. Nagendramma, R. V. Kumar, M. S. S. Kiran, P. Prasad, Durga, A. Leelaratnam, and S. V. K. Varma, *J. Nanofluid* 5, 817 (**2016**).
24. Nagler and Jacob, *J. Nanofluids* 5, 960 (**2016**).
25. O. D. Makinde, S. Das, and R. N. Jana, *J. Nanofluids* 5, 687 (**2016**).
26. A. Pantokratoras and T. Fang, *Phys. Scr.* 87, 015703 (**2013**).
27. T. Hayat, Taseer Muhammad, A. Alsaedi, and M. S. Alhuthali, *J. Magn. Magn. Mater.* 385, 222 (**2015b**).
28. Shehzad Sabir Ali, Tasawar Hayat, Ahmed Alsaedi, and Mustafa Ali Obid, *Appl. Mathematics and Comput.* 248, 273 (**2014**).
29. T. Vijayalaxmi and B. Shanker, *J. Appl. Mathematics and Phys.* 4, 307 (**2016**).
30. M. R. Krishnamurthy, B. C. Prasannakumara, and Rama Subba Reddy Gorla, *J. Nanofluids* 5, 1 (**2016**).
31. Fazle Mabood, Maria imtiaz, Ahmed Alsaedi, and Tasawar Hayat, *PLOs ONE* 17, 221 (**2016**).
32. S. Rosseland, Astrophysik und Atom-theoretischeGrundlagen, Springer, Berlin (**1931**).
33. Shehzad Sabir Ali, *Appl. Mathematics and Comput.* 248, 273 (**2014**).
34. T. Cebeci and P. Bradshaw, Physical and Computational Aspects of Convective Heat Transfer, Springer, Berlin (**1988**).
35. E. Magyari and B. Keller, *J. Phys. D Appl. Phys.* 32, 577 (**2000**).
36. B. Bidin and R. Nazar, *Eur. J. Sci. Res.* 33, 710 (**2009**).
37. M. A. El-Aziz, *Can. J. Phys.* 87, 359 (**2009**).
38. A. Ishak, *Sains Malaysaiana* 40, 391 (**2011**).
39. Swati Mukhopadhyay, *Heat Mass Transfer* 48, 1773 (**2012**).
40. S. Nadeem, S. Zaheer, and T. Fang, *Numer Algor.* (**2011**), DOI: 10.1007/s11075-010-9423-8.

ARTICLE